Natural Resonance Theory: III. Chemical Applications

E. D. GLENDENING,* J. K. BADENHOOP, and F. WEINHOLD**

Theoretical Chemistry Institute and Department of Chemistry, University of Wisconsin, Madison, Wisconsin 53706

Received 15 July 1997; accepted 1 November 1997

ABSTRACT: We describe quantitative numerical applications of the natural resonance theory (NRT) to a variety of chemical bonding types, in order to demonstrate the generality and practicality of the method for a wide range of chemical systems. Illustrative applications are presented for 1) benzene and polycyclic aromatics; 2) CO_2, formate, and related acyclic species; 3) ionic and polar compounds; 4) coordinate covalent compounds and complexes; 5) hypervalent and electron-deficient species; 6) noncovalent H-bonded complex; and 7) a model Diels-Alder chemical reaction surface. The examples exhibit the general harmony of NRT weightings with qualitative resonance-theoretic concepts and illustrate how these concepts can be extended to many new types of chemical phenomena at a quanitative *ab initio* level. © 1998 John Wiley & Sons, Inc. J Comput Chem 19: 628–646, 1998

Keywords: natural resonance theory; resonance theory; bonding; chemical

Introduction

In the two accompanying papers we presented a ''natural resonance theory'' (NRT) algorithm and the associated definitions of NRT bond order and valency indices. In the present paper, we describe quantitative *ab initio* NRT applications to a variety of species in order to demonstrate the generality and practicality of the NRT method for a wide range of chemical systems and to test the consistency of NRT weightings with qualitative Pauling-Wheland[1,2] resonance concepts.

Attempts to apply rigorously the Pauling-Wheland resonance theory were usually limited to the benzene molecule,[3] the prototypical ''resonance hybrid.'' Even before the discovery of quantum theory, it was recognized that the unique properties of benzene (especially its high symmetry and stability) are associated with delocalization of electron-pair bonds from either of the two

*Present address: Department of Chemistry, Indiana State University, Terre Haute, IN 47809

**Present address: Department of Math and Sciences, Potomac State College of West Virginia, Keyser, WV 26726

Correspondence to: F. Weinhold

See the Editor's Note for the first paper in this series, p. 593, this issue.

CCC 0192-8651 / 98 / 060628-19

equivalent Lewis (Kekulé) formulas,

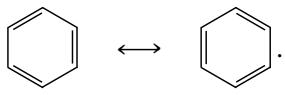

(1.1)

The strongest (''aromatic'') forms of electronic delocalization are sometimes assumed to be restricted to cyclic geometry and symmetry-equivalent resonance structures, as in (1.1), but (as recognized by Pauling and others[4]) similar strong resonance delocalization can occur in species that are acyclic (e.g., CO_2, formate ion) or have unique leading resonance structures (e.g., amide group, naphthalene). Moreover, the well-known instability of cyclobutadiene [despite the superficial ''analogy'' to (1.1)]

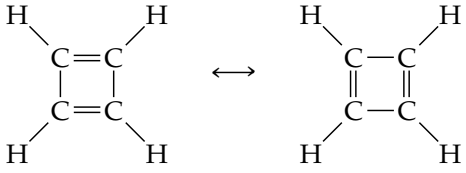

(1.2)

demonstrates that cyclic, symmetry-equivalent structures can *oppose* (rather than promote) resonance stabilization. Thus, a comprehensive theory of quantum-mechanical resonance should describe a wide range of electronic delocalization effects in benzenoid and nonbenzenoid systems, with cyclic or acyclic geometry and equivalent or inequivalent resonance structures.

Several examples of NRT applications to weakly delocalized species (well represented by a conventional Lewis structural formula) were presented in the preceding two papers. In the present paper, we emphasize the applications to strongly delocalized or ''anomalous'' species whose properties cannot be depicted by a conventional Lewis structural formula. Our goal is to present representative examples of NRT applications for a wide range of bonding types, rather than detailed discussion of individual species, providing a baseline for more detailed future investigations. Furthermore, because the two preceding papers describe the numerical stability and convergence of NRT analysis with respect to improvements in theoretical level (extensions of basis, inclusion of correlation effects, etc.), we shall not emphasize this aspect in the present work. Unless otherwise mentioned, all calculations were carried out with default NRT program options. We employ *ab initio* molecular orbital (MO) wave functions at selected basis levels,[5] with either idealized Pople-Gordon[6] or fully optimized geometry, to demonstrate that the analysis is independent of valence bond (VB)-type wave functions.

The plan of the paper is as follows. The next section describes classical cases of resonance in cyclic aromatic benzenoid systems (benzene, naphthalene, anthracene, phenanthrene) and derivatives (toluene, xylenes, benzyl cation). We then describe CO_2, formate, and related strongly delocalized acyclic species (OCNH, HNCNH, allene, formamide, HNO_2, HONO). Next we describe ionic bonding and ''ionic-covalent resonance'' in the series X—F, X—CH_3 (X = Li, CH_3, NH_2, OH, F), examining the transition between covalent and ionic bonding limits. After this we describe coordinate covalent bonding, including Lewis acid-base complexation (BF_3—NH_3) and transition metal coordination (Ni—CO). Later we describe ''octet-violating'' examples of hypervalency (PCl_5, SF_6, SF_4) and electron-deficient hypovalency (B_2H_6, BF_3, F_2CO, F_2N_2). Following this discussion, the next section describes noncovalent bonding, particularly H-bonded complexes (water dimer, cyclic formamide dimer, FHF^-, malonaldehyde), followed by NRT analysis of the potential energy surface for a model Diels-Alder chemical reaction surface, including the ''activated complex'' transition state. The final section presents a brief summary and conclusions.

Cyclic Aromatic Systems

BENZENE AND BENZENE DERIVATIVES

A unique feature of benzenoid systems is the cyclic pattern of conjugation allowing each localized π bond to delocalize into two adjacent π^* antibonds in concerted counterrotating triple cycles.

$$\pi_{AB} \rightarrow \pi^*_{CD}, \pi_{CD} \rightarrow \pi^*_{EF}, \pi_{EF} \rightarrow \pi^*_{AB} \quad (2.1a)$$

$$\pi_{AB} \rightarrow \pi^*_{EF}, \pi_{EF} \rightarrow \pi^*_{CD}, \pi_{CD} \rightarrow \pi^*_{AB} \quad (2.1b)$$

Such concerted donor-acceptor interactions are inherently cooperative, so that each $\pi \rightarrow \pi^*$ interaction of benzene is strengthened relative to a corresponding interaction in, e.g., butadiene. In terms of the resonance-theoretic mnemonic [cf. (4.3) in the first paper], the concerted sequence of 2-*e* delocalizations (2.1a) or (2.1b) leads to the three-bond shifts that convert one Kekulé structure to another. The NRT program[7] automatically searches for Kekulé-like NBO interaction patterns (2.1) whenever strong delocalizations are encountered and

adds the second Kekulé structure if necessary. Note that the cyclic conjugative patterns (2.1) can in principle occur even if the interacting bonds are not linked by a sigma framework [as might occur, e.g., in the transition from localized $(H_2)_3$ to delocalized ''metallic'' H_6 at high pressures],[8] so the reference to a ''Kekulé-like'' structure has only topological significance.

Table I shows the calculated *ab initio* NRT weights for benzene (RHF/6-31G*//PG level). The NRT weights confirm the dominance of the leading Kekulé structures (1.1). A slight admixture (<0.01%) of dipolar ''singly ionic'' structures is associated with individual $\pi_i \rightarrow \pi_j^*$ interactions, according to the standard resonance mnemonic.[9]

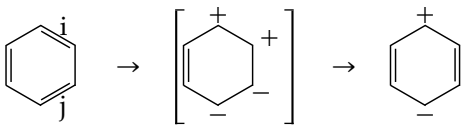

(2.2a)

In terms of Pauling-Wheland ''covalent-ionic resonance,'' this structure could be formally associated with a long-bonded ''Dewar structure'' form

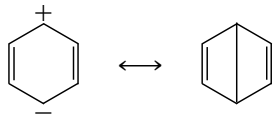

(2.2b)

but this association is unjustified and misleading. The weight of actual Dewar structures in the NRT expansion is negligibly small, apparently owing to a type of numerical ''redundancy'' in the NRT functional (see Appendix). Table I shows that the two Kekulé structures (each 45.8%) essentially dominate the NRT expansion, leading to CC bond orders ($b_{CC} = 1.494$) in excellent agreement with the value ($1\frac{1}{2}$) expected from conventional resonance concepts.[10]

It is interesting to examine the subtle effects of substituents that lift the equivalence of the two leading Kekulé structures and could only be discerned with a quantitative form of resonance theory. From the RHF/6-31G*//PG wave function for toluene, for example, the NRT weights of the two leading[11] resonance structures are found to be (numbers in brackets denote reference structure)

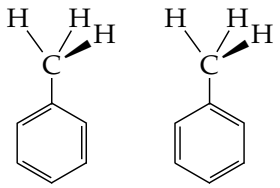

(2.3)

a. [43.8%] b. [42.6%]

showing the slight tendency to ''fix'' the Kekulé structure for which a double bond eclipses the in-plane methyl C—H bond.[12] This leads to slightly higher CC bond order for the 1,6 than for the 1,2 position ($b_{16} = 1.481$, $b_{12} = 1.473$), even in idealized PG geometry. When the ring geometry is optimized, the bonds are found to be slightly distorted in the manner predicted by the bond indices ($R_{16} = 1.3878$ Å, $R_{12} = 1.3926$ Å).

Still more subtle bond-fixing (Mills-Nixon[13]) propensities can be seen in the dimethyl derivatives. For *o*-xylene, the calculated (RHF/6-31G*//PG) NRT weights of the two leading Kekulé structures for the preferred rotamer are

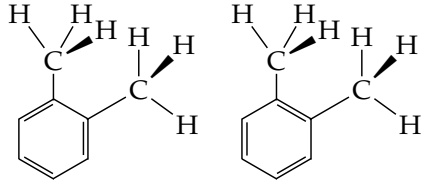

(2.4)

a. [41.7%] b. [40.8%]

and similarly, for *m*-xylene,

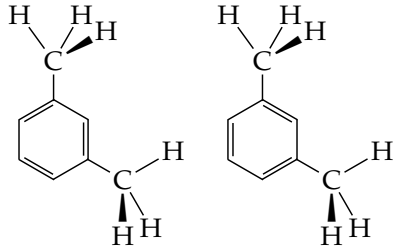

(2.5)

a. [43.2%] b. [41.0%]

and, for *p*-xylene,

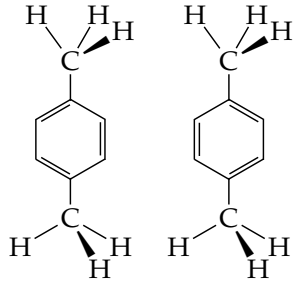

. (2.6)

a. [43.5%] b. [41.2%]

Note that, in all these cases, the energetically preferred rotamer (as shown) allows the in-plane C—H bond of each methyl group to eclipse a π bond of the more highly weighted Kekulé structure. Table II compares the calculated NRT bond orders (for idealized PG geometry) with fully

TABLE I.
Summary of NRT Analysis for RHF/6-31G* Benzene (Pople-Gordon Geometry), Showing Leading Resonance Structure Weightings [w_α; with Degeneracies (Deg.)], Bond Orders (b_{CC}, b_{CH}), and Atomic Valencies (V_C, V_H), with Covalent and Ionic (Electrovalent) Contributions.

Structure α	Deg.	w_α (%)	Structure α	Deg.	w_α (%)
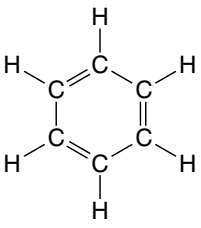	2	45.80	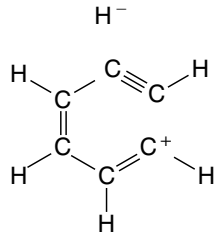	12	0.08
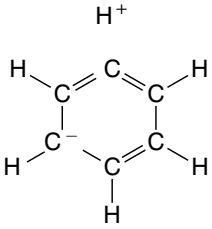	12	0.10	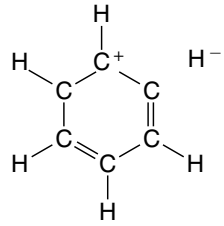	12	0.08
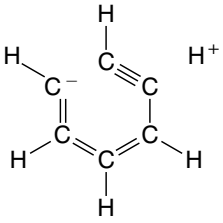	12	0.10	(78 others)		4.08

Atom X	NRT bond order			NRT valency		
	b_{XC}	$b_{XC}^{(cov)}$	$b_{XC}^{(ion)}$	V_X	$V_X^{(cov)}$	$V_X^{(ion)}$
C	1.4941	1.4842	0.0072	3.9706	3.7293	0.2414
H	0.9878	0.7608	0.2270	0.9878	0.7608	0.2270

optimized R_{CC} values for the xylenes and other benzene derivatives, showing that the actual ring distortions are consistent with the calculated variations in NRT weightings. Figure 1 shows the graphical correlation of R_{CC} (optimized) with b_{CC} (PG) for all the neutral aromatic ring bonds (including those discussed in the following subsection), demonstrating the accuracy with which subtle variations of ring geometry [on the order of $\mathscr{O}(10^{-3}$ Å)] are predicted by quantitative NRT bond orders.

As a further test we examine the benzyl cation, which is expected to exhibit much stronger departures from idealized benzene geometry. At the RHF/6-31G*//PG level,[14] the leading NRT resonance structures are[11]

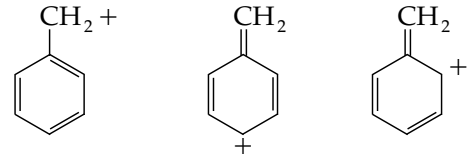

a. [16.2%] (2) b. [11.6%] c. [11.5%] (2) (2.7)

The calculated NRT bond orders predict quinoid-like ring distortion with significant double bond character in the exocyclic CC bond, consistent with experimental findings.[15] Table II includes comparisons of these bond orders with the optimized

TABLE II.

Comparison of Calculated RHF / 6-31G* // PG NRT Bond Orders (b_{CC}, b_{CH}) and Optimized RHF / 6-31G* Bond Lengths (R_{CC}, R_{CH}; in Å) for Benzene Derivatives [see (2.3) – (2.7)]: Benzene; Toluene; Benzyl Cation; *o*-, *m*-, and *p*-Xylene[a]

		Benzene		Toluene		Benzyl cation[b]	
a	b	$b_{ab}^{(PG)}$	$R_{ab}^{(opt)}$	$b_{ab}^{(PG)}$	$R_{ab}^{(opt)}$	$b_{ab}^{(PG)}$	$R_{ab}^{(opt)}$
C_1	C_2	1.4941	1.3862	1.4648	1.3926	1.2243	1.4365
C_2	C_3	1.4941	1.3862	1.4938	1.3830	1.5075	1.3621
C_3	C_4	1.4941	1.3862	1.4807	1.3875	1.3715	1.4030
C_4	C_5	1.4941	1.3862	1.4913	1.3829	1.3715	1.4030
C_5	C_6	1.4941	1.3862	1.4773	1.3879	1.5075	1.3621
C_6	C_1	1.4941	1.3862	1.4810	1.3878	1.2243	1.4365
C_1	C_x	—	—	1.0081	1.5115	1.4867	1.3577
C_2	H	0.9878	1.0756	0.9872	1.0769	0.9874	1.0747
C_3	H	0.9878	1.0756	0.9879	1.0758	0.9878	1.0727
C_4	H	0.9878	1.0756	0.9877	1.0754	0.9880	1.0752
C_5	H	0.9878	1.0756	0.9879	1.0758	0.9878	1.0727
C_6	H	0.9878	1.0756	0.9872	1.0763	0.9874	1.0747
C_x	H_i	—	—	0.9975	1.0838	0.9982	1.0751
C_x	H_o	—	—	0.9904	1.0860	—	—

		o-Xylene		*m*-Xylene		*p*-Xylene	
a	b	$b_{ab}^{(PG)}$	$R_{ab}^{(opt)}$	$b_{ab}^{(PG)}$	$R_{ab}^{(opt)}$	$b_{ab}^{(PG)}$	$R_{ab}^{(opt)}$
C_1	C_2	1.4542	1.4012	1.4596	1.3949	1.4597	1.3944
C_2	C_3	1.4727	1.3874	1.4867	1.3841	1.4937	1.3796
C_3	C_4	1.4778	1.3866	1.4625	1.3946	1.4597	1.3944
C_4	C_5	1.4935	1.3809	1.4979	1.3792	1.4878	1.3839
C_5	C_6	1.4778	1.3866	1.4754	1.3895	1.4700	1.3900
C_6	C_1	1.4727	1.3874	1.4881	1.3841	1.4878	1.3840
C_1	C_x	1.0076	1.5118	1.0082	1.5115	1.0080	1.5112
$C_{2,3,4}$	C_y	1.0076	1.5118	1.0082	1.5114	1.0080	1.5112
C_2	H	—	—	0.9867	1.0776	0.9874	1.0771
C_3	H	0.9873	1.0763	—	—	0.9874	1.0771
C_4	H	0.9878	1.0756	0.9872	1.0767	—	—
C_5	H	0.9878	1.0756	0.9880	1.0759	0.9874	1.0765
C_6	H	0.9873	1.0763	0.9872	1.0761	0.9874	1.0764
C_x	H_i	0.9977	1.0835	0.9976	1.0838	0.9975	1.0839
C_x	H_o	0.9903	1.0863	0.9903	1.0860	0.9904	1.0861
C_y	H_i	0.9977	1.0835	0.9976	1.0838	0.9975	1.0839
C_y	H_o	0.9903	1.0863	0.9904	1.0860	0.9904	1.0861

[a]Carbon atoms are labelled as shown below.

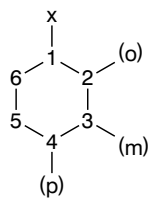

H_i, H_o, respectively, denote in-plane and out-of-plane H atoms (with H_i *cis* to C_6), and C_y denotes the second methyl carbon (C_o, C_m, or C_p) in the xylenes.

[b]PG geometry.

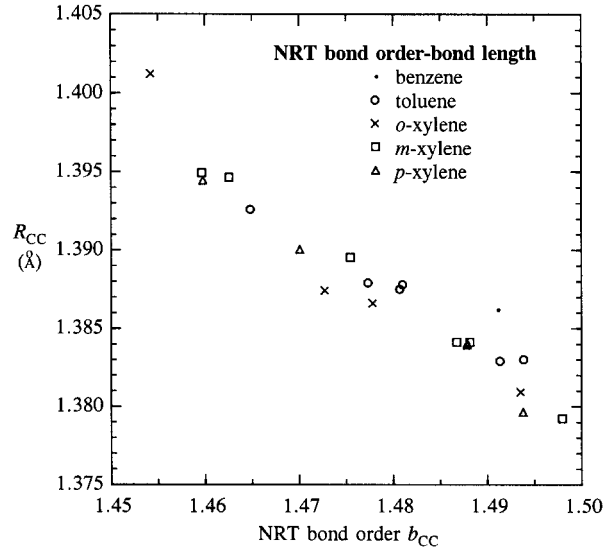

FIGURE 1. NRT bond order–bond length correlation for neutral aromatic ring CC bonds of Table II, comparing bond orders of idealized geometry (all R_{CC} = 1.40 Å) to the fully optimized bond lengths: benzene (dot), toluene (circles), *o*-xylene (crosses), *m*-xylene (squares), and *p*-xylene (triangles).

bond lengths,[16] showing the correlation with the actual distortions.

Whereas the $\pi_i \rightarrow \pi_j^*$ interactions of benzene and other aromatics give rise to strong stabilizing delocalizations and alternative resonance structures, the corresponding delocalizations in cyclobutadiene (1.2) are wholly absent. This is due to the fact that the near-rectangular geometry of a hypothetical closed-shell cyclobutadiene molecule necessarily puts the localized π and π^* orbitals in a nearly *parallel* arrangement, so that the nodal plane of the antibonding π^* leads to effective cancellation of $\pi_i - \pi_j^*$ overlap (and Fock matrix element, etc.). Hence, the alternative resonance structure shown in (1.2) gains no weighting in the NRT expansion, and the cyclobutadiene molecule gains none of the conjugative delocalization that usually stabilizes species with adjacent double bonds.

POLYCYCLIC AROMATICS

We also briefly illustrate application of the NRT method to polycyclic aromatic systems (all calculated at the split valence RHF/3-21G//PG level). For these examples we set NRTTHR = 10 (i.e., increase the threshold for estimated second-order resonance stabilization energy from 1 to 10 kcal/mol) to suppress the many structures associated with weak sigma delocalization.

For naphthalene, the leading NRT weightings are found to be

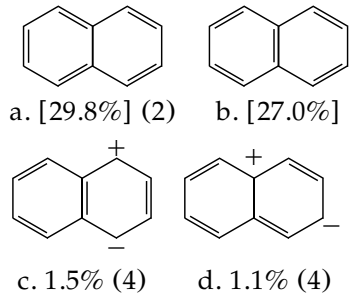

(2.8)

Note that the high weight of the nondegenerate resonance structure (2.8b) implies a significantly higher degree of pi bond fixation in naphthalene than in benzene. Table III compares the calculated NRT bond orders (for the idealized PG geometry with all CC bonds fixed at 1.40 Å) to fully optimized CC bond lengths, which are seen to exhibit the expected pattern of distortions. Graphical representations of these correlations are displayed in Figure 2.

We also consider two fused three-ring $C_{14}H_{10}$ isomers, anthracene and phenanthrene, at the RHF/3-21G//PG level. For anthracene, the leading NRT structures are found to be

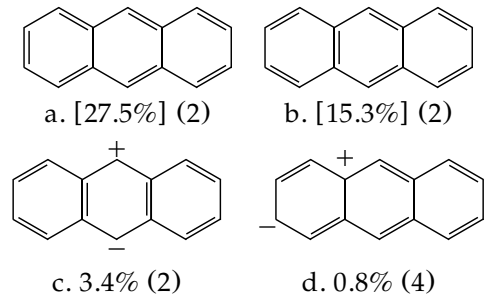

(2.9)

Similarly, NRT analysis for phenanthrene gives

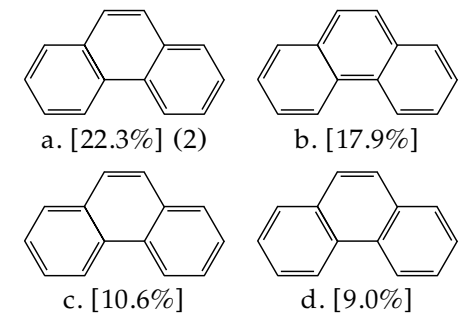

(2.10)

TABLE III.

Comparison of Calculated RHF/3-21G//PG NRT Bond Orders ($b_{ij}^{(PG)}$) and Optimized RHF/3-21G Bond Lengths ($R_{ij}^{(opt)}$, in Å) for C_i—C_j Bonds of Naphthalene, Anthracene, and Phenanthrene [See Eq. (2.8)–(2.10)], with the Atom Numberings Shown Below.[a]

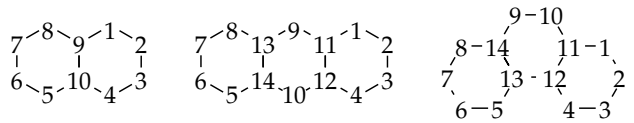

	Naphthalene	Anthracene		Phenanthrene			
i	j	$b_{ij}^{(PG)}$	$R_{ij}^{(opt)}$	$b_{ij}^{(PG)}$	$R_{ij}^{(opt)}$	$b_{ij}^{(PG)}$	$R_{ij}^{(opt)}$
1	2	1.6441	1.3569	1.6996	1.3645	1.5892	1.3646
1	9	1.3218	1.4186	—	—	—	—
2	3	1.3368	1.4143	1.2881	1.4301	1.3941	1.3998
9	10	1.3279	1.4086	—	—	1.7479	1.3370
1	11	—	—	1.2907	1.4343	1.3770	1.4063
9	11	—	—	1.4620	1.3874	—	—
11	12	—	—	1.2354	1.4243	1.3811	1.4036
3	4	—	—	—	—	1.5890	1.3667
4	12	—	—	—	—	1.3929	1.4086
10	11	—	—	—	—	1.2216	1.4389
12	13	—	—	—	—	1.2036	1.4604

[a]Note that the CC, CH bonds of polycyclic aromatics are all assumed equal to corresponding benzene values (1.40 Å, 1.08 Å) in idealized PG geometry, so that the calculated $b_{ab}^{(PG)}$ values reflect intrinsic electronic differences rather than variations in bond lengths.

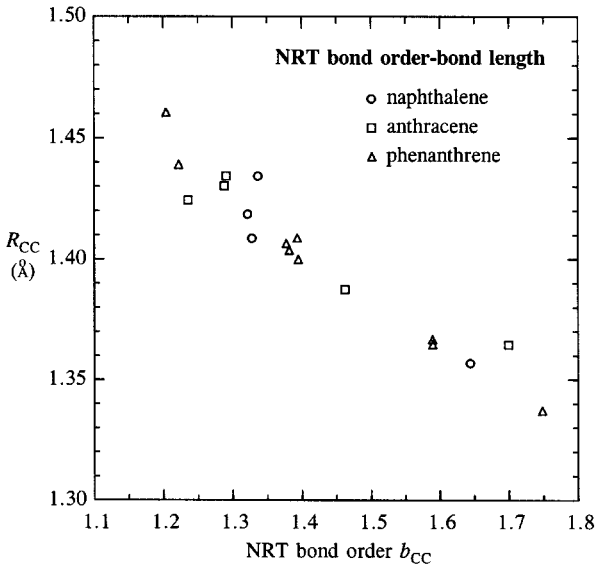

FIGURE 2. Similar to Figure 1, for polycyclic aromatics of Table III: naphthalene (circles), anthracene (squares), and phenanthrene (triangles).

with lesser contributions from many ionic structures. Table III includes comparisons of (idealized PG) NRT bond orders with optimized CC bond lengths for all these species, showing the overall pattern of agreement (despite the severe constraints of ring geometry). Figure 2 exhibits the graphical bond order–bond length correlation for the polycyclic aromatics over the full range of CC variation from near-single to near-double bond character. The NRT results appear to be in satisfactory overall harmony with qualitative resonance-theoretic concepts of organic chemistry,[17] but the NRT weightings bring out many subtleties of resonance delocalization that would not be apparent in the qualitative framework.

Carbon Dioxide, Formate Ion, and Related Acyclic Species

CO_2 AND RELATED SPECIES

A particularly interesting type of acyclic strong delocalization is exhibited by the carbon dioxide molecule, which Pauling judged to have equal resonance contributions from the double-bonded and triple-bonded forms.[18] In the nominal Lewis representation (:Ö═C═Ö:), there are strong $n_O \rightarrow \pi^*_{CO}$ delocalizations in the orthogonal pi systems of each of the two (degenerate) NBO Lewis structures. In excellent accordance with Pauling's description are comparable NRT contributions (RHF/6-31G*//PG level) from double- and

triple-bonded resonance structures,[9]

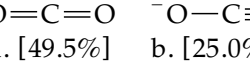

(3.1)

The resonance-weighted NRT bond orders (b_{CO} = 2.000) essentially coincide with classical structural formulas, even though NBO analysis indicates that strong $n_O \rightarrow \pi^*_{CO}$ delocalizations (each estimated at 199 kcal/mol by second-order perturbation theory) make each CO bond quite unlike that of, e.g., formaldehyde.

The strong $n \rightarrow \pi^*$ delocalizations can be successively removed by ''protonating'' each lone pair and decreasing nuclear charge to preserve neutrality in the isovalent sequence O=C=O, HN=C=O...H_2C=C=CH_2. Each such replacement diminishes the weight of a triple-bonded form (arising from $n \rightarrow \pi^*$ delocalization). The first of these ''partially localized'' analogs, HN=C=O, has NRT weightings

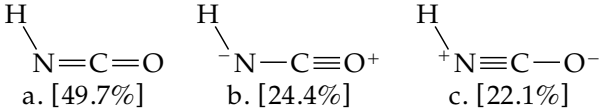

(3.2)

reflecting the ''symmetry breaking'' of the two orthogonal pi systems. The next member, HN=C=NH, has a twisted symmetric (S_2) structure with NRT weightings reflecting still higher pi localization,

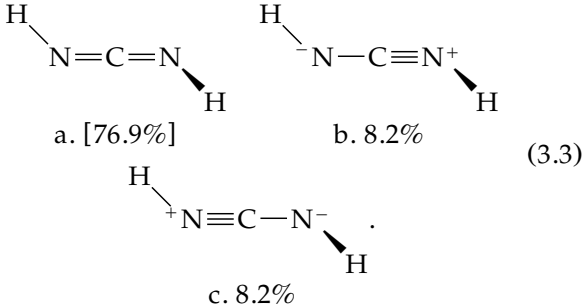

(3.3)

Finally in allene, in which the last of the $n \rightarrow \pi^*$ delocalizations is removed, only the nominal double-bonded resonance structure has significant weighting (91.9%). Thus, the NRT weightings[19] exhibit the expected successive degrees of localization of the pi system in this isovalent sequence.

FORMATE ION AND RELATED SPECIES

It is also interesting to consider the general A=B—C̈ ''keto-enol'' resonance motif,

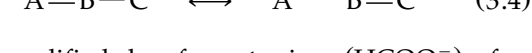

(3.4)

as exemplified by formate ion ($HCOO^-$), formamide (H_2NCHO), nitrous acid (HONO), HNOO, and other species. We describe NRT applications to several such systems at the geometry-optimized RHF/6-31 + G* level of theory.

The formate ion itself is a classic case of strong, symmetric delocalization, with equivalent leading NRT structures

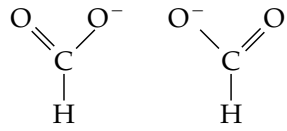

(3.5)

and equal CO bond orders (b_{CO} = 1.524) of significant ionic character ($b_{CO}^{(ion)}$ = 0.689, $b_{CO}^{(cov)}$ = 0.835).[20] An analogous neutral pattern is seen in HNO_2,

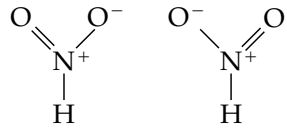

(3.6)

with similar NO bond orders (b_{NO} = 1.518) and even higher ionicity ($b_{NO}^{(ion)}$ = 1.226, $b_{NO}^{(cov)}$ = 0.296).

The corresponding nonsymmetric pattern is exemplified by the amide group[21] of formamide, which has leading NRT structures

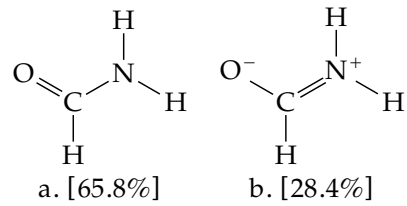

(3.7)

with distinct CO and CN bond orders (b_{CO} = 1.744, b_{CN} = 1.289) and degrees of ionicity ($b_{CO}^{(ion)}$ = 0.715, $b_{CO}^{(cov)}$ = 1.029; $b_{CN}^{(ion)}$ = 0.508, $b_{CN}^{(cov)}$ = 0.781). Similarly, the NRT weightings for HONO

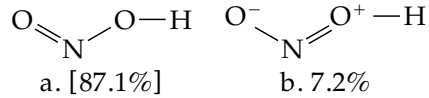

(3.8)

result in nonsymmetric NRT bond orders (protonated $b_{NO} = 1.042$, free $b_{NO} = 1.968$), reflecting the still greater dominance of the leading resonance structure.[19] The greater weighting of the dipolar structure in formamide (3.7b) than in HONO (3.8b) can be attributed to the better donor (Lewis base) character of n_N vs. n_O (i.e., greater electropositivity of N) and better acceptor (Lewis acid) character of π^*_{CO} vs. π^*_{NO} (i.e., greater CO electronegativity difference polarizing the pi antibond toward the central atom), leading to stronger $n_N \rightarrow \pi^*_{CO}$ than $n_O \rightarrow \pi^*_{NO}$ NBO delocalizations. Thus, the relative NRT weights in (3.7) and (3.8) seem to be in agreement with expected chemical trends.

Ionic Bonding and "Ionic-Covalent Resonance"

The description of ionic and polar compounds presents a peculiar difficulty in Pauling-Wheland resonance theory, insofar as it was necessary to attribute "covalent" and "ionic" resonance structures to molecules that were conventionally described by a single Lewis structure formula. This difficulty stems from the fact that the Heitler-London VB pair function describes homopolar bonds ("pure covalent" bonding), so that bond polarity must be represented with "ionic-covalent resonance."[22] No such difficulty arises in the NBO/NRT formalism; each two-center polar bond (e.g., $\sigma_{AB} = c_A h_A + c_B h_B$) can vary continuously between homopolar ($c_A = c_B$) and ionic ($c_A = 0$ or $c_B = 0$) limits within the framework of a *single* localized Lewis structure formula.

To illustrate the distinctive treatment of ionic or polar covalent bonding in the NRT framework, we consider two series of molecules,

$$\left.\begin{matrix} X\text{—}F \\ X\text{—}CH_3 \end{matrix}\right\} X = Li,\ CH_3,\ NH_2,\ OH,\ F. \quad (4.1)$$

As expected, these are all well described by a single NRT structure (>99%). Table IV displays the calculated X—F and X—C bond orders (b_{XF}, b_{XC}), as well as their ionic ($b^{(ion)}_{XF}$, $b^{(ion)}_{XC}$) and covalent ($b^{(cov)}_{XF}$, $b^{(cov)}_{XC}$) components, at the RHF/6-31G*//PG level.

As Table IV shows, the formal X—F or X—C bond order is always close to unity (1.01 ± 0.01), corresponding to the nominal single bond of the coventional Lewis structure. However, the bond type ranges from nearly pure ionic (e.g., $b^{(ion)}_{XF} \simeq 1$, $b^{(cov)}_{XF} \simeq 0$ for X = Li) to covalent (e.g., $b^{(ion)}_{XF} = 0$, $b^{(cov)}_{XF} = 1$ for X = F). The NRT ionic and covalent bond orders are seen to vary smoothly in the manner expected from empirical electronegativity differences.

It is noteworthy that (except for X = Li) the methyl C—X bonds exhibit slight partial double bond character, of the type expected to give rise to torsional barriers. The resonance structures responsible for partial C = X character are associated with hyperconjugative $\sigma \rightarrow \sigma^*$ (or $n \rightarrow \sigma^*$) interactions that were previously identified[23] as the principal origin of barriers to internal rotation in ethane-like molecules. Weak resonance delocalization of the form

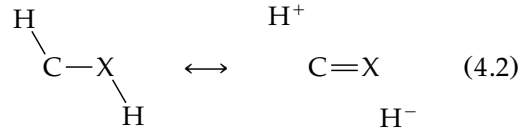

(4.2)

can therefore be considered as the resonance-theoretic counterpart of the $\sigma \rightarrow \sigma^*$ "charge transfer" picture.[24] The somewhat surprising *ionic* contribution to CC bonding in ethane ($b^{(ion)}_{CC} = 0.019$, corresponding to about 2% ionic character) can also be attributed to the dipolar hyperconjugative structures in (4.2).

Table IV also shows the variations in NRT covalency ($V^{(cov)}_F$, $V^{(cov)}_C$), electrovalency ($V^{(ion)}_F$, $V^{(ion)}_C$), and total atomic valency (V_F, V_C) for F and C atoms. Consistent with standard valence concepts, fluorine is found to be essentially "univalent" ($V_F = 1.00 \pm 0.02$) and carbon "tetravalent" ($V_C = 4.000 \pm 0.004$) in all these compounds. The covalency of F (or C) is found to vary steadily with the F—X (or C—X) electronegativity difference in the expected way. Thus, the NRT description of ionic and polar compounds bypasses the problematic "ionic-covalent resonance" of Pauling-Wheland theory but achieves very satisfactory agreement with intuitive electronegativity and valency concepts that underlie Pauling's classic description of chemical bonding.[4]

Coordinate Covalent Bonding: Lewis Acid–Base and Organometallic Complexes

Coordinate covalency ("dative" or "donor-acceptor" bonding) represents a pervasive bonding

TABLE IV.
Variations in NRT Bond Order and Atomic Valency [and Their Covalent and Ionic Contributions: $V_F^{(cov)} = C_F$, $V_F^{(ion)} = E_F$; See Eq. (2.12) in the Preceding Paper] in a Series of X—F and X—CH_3 Compounds (X = Li, CH_3, NH_2, OH, F), Evaluated at RHF / 6-31G* // PG Level (Except for X = Li, Where Geometry Was Optimized).

	X—F compounds							X—CH_3 compounds						
	NRT bond order (X—F)				NRT atomic valency (F)			NRT bond order (X—C)				NRT atomic valency (C)		
X	b_{XF}	$b_{XF}^{(cov)}$	$b_{XF}^{(ion)}$	% Ionic	V_F	$V_F^{(cov)}$	$V_F^{(ion)}$	b_{XC}	$b_{XC}^{(cov)}$	$b_{XC}^{(ion)}$	% Ionic	V_C	$V_C^{(cov)}$	$V_C^{(ion)}$
Li	1.000	0.026	0.974	97.4	1.000	0.026	0.974	1.000	0.135	0.865	86.5	4.000	1.388	2.613
CH_3	1.019	0.526	0.493	48.4	1.019	0.526	0.493	1.019	1.000	0.019	1.9	4.000	3.346	0.654
NH_2	1.006	0.691	0.315	31.3	1.006	0.691	0.315	1.023	0.801	0.222	21.7	4.000	3.181	0.819
OH	1.000	0.836	0.163	16.3	1.000	0.836	0.163	1.022	0.645	0.377	36.9	4.000	3.060	0.940
F	1.000	1.000	0.000	0.0	1.000	1.000	0.000	1.019	0.507	0.493	48.4	3.996	2.970	1.026

motif in many inorganic and organometallic species.[25] Formation of a coordinate bond between a Lewis base ''donor'' and Lewis acid ''acceptor'' leads to a special type of polar covalency whose NRT description resembles that of ionic and strong polar covalent bonding, as discussed in the preceding section.

To illustrate the application of NRT to coordinate complexes, we consider the prototype Lewis acid–base adduct $BF_3 \cdots NH_3$ (geometry optimized RHF/6-31G* level), whose leading NRT weightings are shown below.

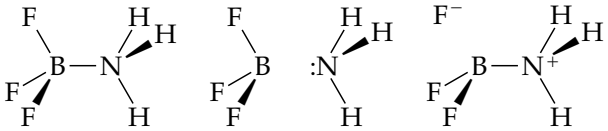

a. [35.8%] b. [14.9%] c. [12.3%] (3)

(5.1)

The coordinate B ⋯ N bond is found to have total bond order $b_{BN} = 0.803$ of high polarity ($b_{BN}^{(ion)} = 0.589$). Note that formation of the final acid–base adduct from its isolated Lewis base ($:NH_3$) and Lewis acid (BF_3) precursors involves promotion of the B—N bonded resonance structure (5.1a) from a minor secondary structure at large separation to the leading reference structure at equilibrium, so the NRT weightings will exhibit a ''discontinuity'' (of the type described in the preceding paper) at some intermediate distance unless both structures (5.1a, b) are stipulated as reference structures for all R (cf. penultimate section).

As a second example, we consider the nickel carbonyl complex, NiCO. The wave function was taken to be of RHF/LANL1DZ form (Hay-Wadt double zeta ECP basis),[26] with equilibrium bond lengths $R_{NiC} = 1.7696$ Å and $R_{CO} = 1.1483$ Å. NRT analysis of this wave function leads to the resonance weightings

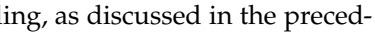

a. [87.4%] b. 12.4% c. 0.2% .

(5.2)

With respect to Ni and CO precursors, structure (5.2a) is due to carbonyl lone pair donation into unfilled Ni valence orbitals and (5.2b) to π back-bonding from metal d into unfilled carbonyl π_{CO}^* orbitals. Note that (5.2c) represents the carbonyl moiety as double bonded (formally, ''octet violating'' at C), rather than the usual triple-bond ''free'' CO. The calculated NRT bond orders indicate that the coordinate NiC bond (with $b_{NiC} = 1.122$) has high polarity (86.1% ionic character), and the carbonyl bond order ($b_{CO} = 2.874$) is significantly reduced from its value in free CO. These NRT weightings and bond orders appear to be in good overall agreement with conventional concepts of bonding in Werner-type complexes.[27]

''Octet Rule-Violating'' Hypervalent and Hypovalent Bonding

The NRT structures of most stable compounds appear to conform well to the Lewis octet rule. However, NRT analysis can also be applied to species exhibiting formal surplus (''hypervalency'') or deficiency (''hypovalency'') of valence electron pairs. In the former case, the NRT program can

recognize hypervalency if the number of formal electron pairs of a candidate structure exceeds the valence shell dimensionality, and multireference weighting (if required) is then carried out in the full NAO basis rather than the restricted valence space. We briefly present numerical examples for each of these exceptional bonding types.

"HYPERVALENT" SPECIES

A classical example of hypervalency is "pentavalent" PCl_5, in which P appears to be surrounded by five valence electron pairs.[28] NRT analysis of the geometry-optimized RHF/6-31G* wave function for this species gives the six reference structures shown below.

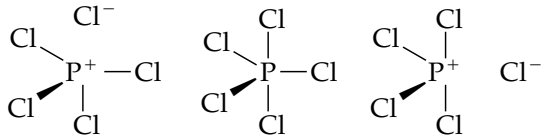

a. [18.1%] (2) b. [12.4%] c. [10.2%] (3) (6.1)

Each PCl bond [with $b_{PCl} = 0.744$ (*ax*) and 0.849 (*eq*)] is of rather high ionic character [41.1% (*ax*), 34.2% (*eq*)]. As is shown in (6.1), five of the leading resonance structures (accounting for about 67% of the NRT expansion) are found to obey the octet rule, and the calculated atomic valency of phosphorus ($V_P = 4.036$, $V_P^{(cov)} = 2.554$) appears only slightly exceptional. Evidently, the high ionic character of P—Cl bonding permits high coordination number to phosphorus within the constraint of the octet rule.

Another classical example of apparent hypervalency is given by sulfur hexafluoride, SF_6.[29] At the RHF/6-31G* geometry-optimized level, SF_6 gives rise to the 16(!) reference structures shown below:

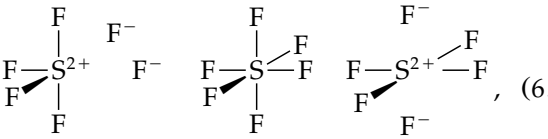

a. [6.3%] (12) b. [5.4%] [3.5%] (3) (6.2)

only one of which [(6.2b), approximately 5%] is formally hypervalent.[30] The formal SF bond orders are all equal ($b_{SF} = 0.680$) and of high polarity ($b_{SF}^{(ion)} = 0.419$). Although the total atomic valency of sulfur ($V_S = 4.080$) is rather unusual, the calculated NRT covalency ($V_S^{(cov)} = 1.564$) is actually less than expected for a nominal "divalent" element (and far less than the apparent "hexavalency" of a superficial line formula). With respect to the charge distributions as well as the relative unimportance of *d*-orbital participation, the NRT results are quite consistent with the NBO analysis presented by Reed,[29] showing the close connection between these descriptions.

As a final example, we consider SF_4 ("sawhorse" geometry, C_{2v}). At the geometry-optimized RHF/6-31G* level, the two sets of SF bonds are inequivalent, leading to the five reference structures shown below.

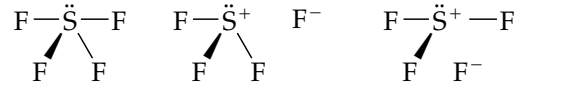

a. [21.1%] b. [19.8%] (2) c. [14.0%] (2) (6.3)

The near-collinear SF bonds have lower total b_{SF} (0.772 vs. 0.820) but higher $b_{SF}^{(ion)}$ (0.534 vs. 0.489) than do the two transverse bonds, consistent with an ionic picture of linear three-center hypervalent bonds[28] (also applicable to the bonding in SF_6[29]). Although leading structure (6.3a) is formally hypervalent, the other four reference structures (accounting for about 67% of the NRT expansion) are not, and neither the sulfur total valency ($V_S = 3.184$) nor the covalency ($V_S^{(ion)} = 1.138$) suggests the five valence electron pairs that might be naively inferred from a line formula. Further aspects of hypervalency in relation to NRT weightings and natural charge distributions are discussed elsewhere.[31]

"HYPOVALENT" (ELECTRON-DEFICIENT) SPECIES

A classical example of electron-deficient bonding is diborane,[32] B_2H_6, which leads (at geometry-optimized RHF/6-31G* level) to the NRT weightings shown below.

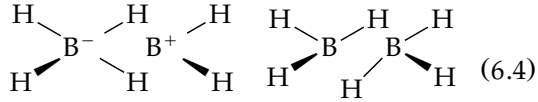

a. [25.1%] (2) b. [24.3%] (2) (6.4)

In the NRT representation, the bridging BH bonds have significantly lower bond order ($b_{BH} = 0.500$)

and higher polarity ($b_{BH}^{(ion)} = 0.221$) than do the ''ordinary'' flanking BH bonds ($b_{BH} = 0.995$, $b_{BH}^{(ion)} = 0.024$). Note that this molecule is well described by a single NBO structure with two three-center B—H—B bonds, and the NRT weightings and bond orders from (6.4) are crudely consistent with Pauling's standard resonance-theoretic treatment of three-center bridge bonds.[33] The calculated NRT atomic valency of boron ($V_B = 2.943$) is in excellent agreement with the empirical trivalency of Group III elements.

A still simpler type of hypovalency is represented by the Lewis acid BF_3 [cf. (5.1)], whose NRT representation (geometry-optimized RHF/6-31G* level) has leading structures

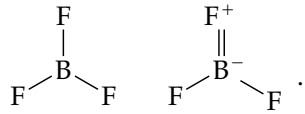

a. [76.1%] b. 5.2% (3) (6.5)

The dipolar structures in (6.5) lead to B—F bonds with partial double-bond character ($b_{BF} = 1.050$) and high ionicity ($b_{BF}^{(ion)} = 0.774$). The total natural valency of boron ($V_B = 3.150$) is seen to be primarily of electrovalent origin ($V_B^{(ion)} = 2.201$), and the leading resonance structure (6.5a) is indeed of ''octet-violating'' form.

It is interesting to compare BF_3 with the isoelectronic species F_2CO and F_2NN (at the same RHF/6-31G* level). The leading NRT structures of F_2CO are found to be

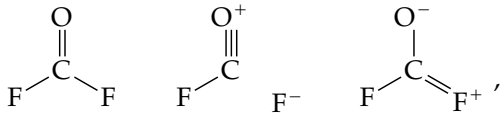

a. [51.0%] b. [18.9%] (2) c. 2.6% (2) (6.6)

with bond orders ($b_{CO} = 2.335$, $b_{CF} = 0.821$) of relatively high ionic character ($b_{CO}^{(ion)} = 1.046$, $b_{CF}^{(ion)} = 0.441$), having somewhat higher b_{CO} than formaldehyde (2.045). The corresponding NRT representation of F_2NN is

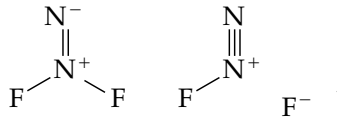

a. [46.4%] b. [23.4%] (2) (6.7)

with increased NN triple-bond character ($b_{NN} = 2.473$, $b_{NN}^{(ion)} = 0.808$) and weaker NF bonds ($b_{NF} = 0.742$, $b_{NF}^{(ion)} = 0.176$). Thus, these isoelectronic AXF_2 species illustrate the progressive change in AX bonding from ''single'' (A = B, X = F) to ''double'' (A = C, X = 0) to ''triple'' (A = X = N), in accordance with conventional Lewis structure models.

Noncovalent Bonding: H-Bonded Complexes

The topic of ''noncovalent'' hydrogen bonding is of special interest for resonance theory. Pauling[34] originally judged that the H-bond was esentially of pure electrostatic rather than ''partial divalent'' character (as had been suggested by Lewis[35]). However, Sidgwick[36] applied the theory of resonance to H bonding, and Coulson[37] concluded that resonance effects were the leading contributions to H bond attraction. The controversy regarding whether H bonding is primarily of ''electrostatic'' or ''resonance'' (partial covalent) nature has continued unabated.[38] Although the original resonance picture of A—H ⋯ B hydrogen bonding [cf. (3.4)]

$$A—H\ :B \longleftrightarrow A:^{-}\ H—B^{+} \qquad (7.1)$$

was developed by Sidgwick (rather than Pauling and Wheland), we can compare NRT applications with this conventional Pauling-Wheland-like resonance description.

We first consider the elementary example of the water dimer, $(H_2O)_2$, at the optimized RHF/6-31 + G* level. NRT analysis leads to the leading resonance structures

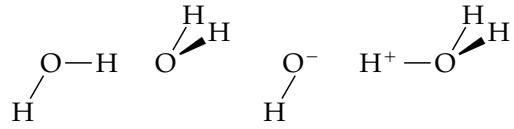

a. [98.1%] b. 1.9% (7.2)

Consistent with (7.1), the NRT expansion predicts appreciable O ⋯ H bond order ($b_{OH} = 0.019$). The appearance of the ''ion pair'' contribution (7.2b) is consistent with the suggestion of significant ''charge transfer'' character of the H-bonded complex.[39]

The H-bonded complex F^- ⋯ HF demonstrates another aspect of intermolecular resonance delocalization, in that the resonating contributions analogous to (7.1) are symmetrically related,

$$F—H\ \ F^{-} \longleftrightarrow F^{-}\ \ H—F, \qquad (7.3)$$

and the equilibrium geometry is *symmetric* ($D_{\infty h}$), suggesting the analogy with CO_2, formate ion, and other cases of symmetric strong delocalization. As expected, the NRT expansion for this species (RHF/6-31G* level) is dominated (50.0% each) by the two structures in (7.3), and both partial FH bonds ($b_{FH} = 0.500$) have significant covalent ($b_{FH}^{(cov)} = 0.106$) and ionic ($b_{FH}^{(ion)} = 0.394$) bonding character. As with other symmetric and unsymmetric examples discussed in previous sections, the resonance contributions in (7.2) and (7.3) appear to differ in degree, but not in type.

Another interesting aspect of intermolecular H bond resonance is its ability to *couple* to *intramolecular* resonance delocalization. This can be illustrated with the example of the formamide dimer, $(NH_2CHO)_2$, cyclically H bonded. At the same RHF/6-31 + G* level used for formamide [cf. (3.7)], the NRT expansion for the cyclic dimer has the leading terms

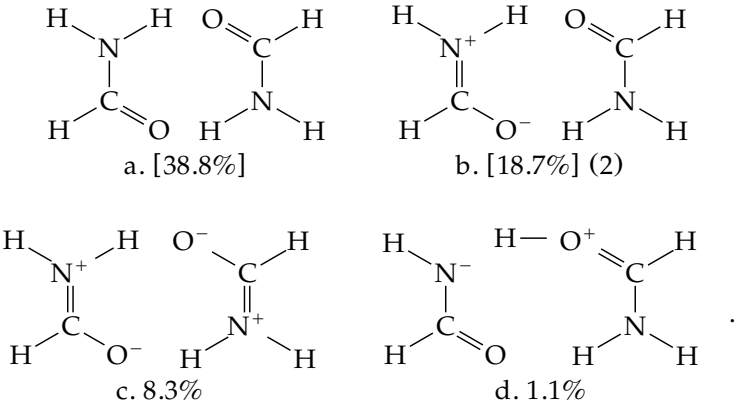

(7.4)

In addition to the leading H-bonded structure (7.4d), other structures appear in which H-bonding is coupled to the $n_N \rightarrow \pi^*_{CO}$ delocalization (totalling about 3.3%), giving rise to appreciable bond order ($b_{O\cdots H} = 0.027$) in each H bond. As expected, dipolar amide resonance structures (7.4b, c) are the leading delocalizations, but it is noteworthy that their relative weighting is significantly *greater* than that in the monomer. The calculated dimer bond orders $b_{CN} = 1.307$ and $b_{CO} = 1.718$ (cf. $b_{CN} = 1.292$ and $b_{CO} = 1.744$ for the monomer) also reflect the enhanced amide resonance. From such comparisons one can recognize that amide delocalization is significantly strengthened by dimer formation, i.e., that H bond formation couples with, and *enhances*, amide resonance (and vice versa). Such coupling effects can be anticipated from the donor-acceptor character of H bonding.[38,39]

Finally, we consider the case of *intramolecular* H bonding in methylated malonaldehyde[40] (optimized RHF/6-31 + G* level), for which the leading NRT structures are

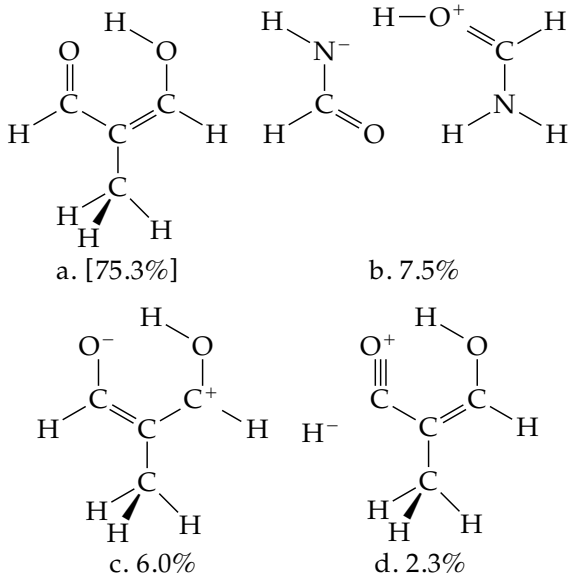

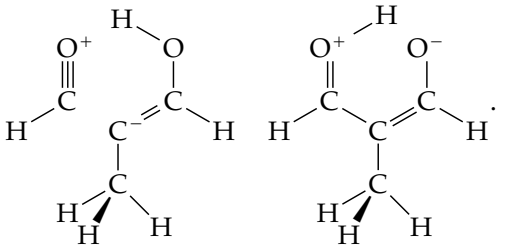

e. 1.7% f. 1.3% (7.5)

Structures (7.5b, c) are associated with expected pi conjugation ($\pi_{CO} \rightarrow \pi^*_{CC}$, $\pi_{CC} \rightarrow \pi^*_{CO}$) and (7.5d, e) with weaker sigma conjugation around the carbonyl group ($n_O \rightarrow \sigma^*_{CH}$, $n_O \rightarrow \sigma^*_{CC}$), whereas (7.5f) is the expected H bonding resonance, analogous to that found previously [e.g., (7.2b)] in the intermolecular case. As with (7.4), one would expect that π-conjugative and H bond resonance would be coupled (and mutually enhanced) as the proton shifts from one oxygen toward the other. [Note, however, that even a symmetrically bridged O···H···O species will exhibit slight differences between the weightings for the two ''equivalent'' (O H—O ↔ O—H O) tautomeric forms, owing to methyl-eclipsing effects analogous to those in (2.3)–(2.6).] Quantitative aspects of the well-known ''proton hopping''[41] dynamics of malonaldehyde and related species should be reflected in the NRT weightings.

Chemical Transformation on a Potential Energy Surface: Reactant, Product, and Transition Species

As a final example, we consider the NRT representation of a model Diels-Alder chemical reaction,

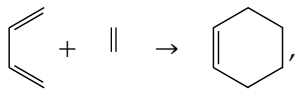 (8.1)

to illustrate the use of user-selected reference structures to compare widely differing reactant (R) and product (P) systems. We employ a model reaction coordinate (s) corresponding to the distance from the ethylene CC midpoint to the point midway between the terminal C atoms of *cis*-butadiene in constrained C_s symmetry. For each value of s, the remaining bond distances and angles were optimized (C_s constrained) at the RHF/3-21G level. Although several aspects of this model are idealized with respect to actual Diels-Alder reactions, the calculated reaction energy profile (Fig. 3a) shows the expected qualitative features, with the separated reactant state at the left (ethylene + butadiene, initially at $s_R = 3.0$ Å) leading to the final product state at the right (equilibrium cyclohexene, at $s_P = 1.4324$ Å), separated by an activated ''transition state'' (at $s^\ddagger = 2.0945$ Å).

To compare the weightings of reactant-like (w_R) and product-like (w_P) resonance structures across the entire reaction coordinate, we stipulate (with the $NRTSTR keylist) that these two resonance structures be considered as reference structures at all s (despite the small weight of w_R in the P region and vice versa). Figure 3b shows the calculated NRT values of w_R and w_P along the reaction coordinate. As expected, the R structure dominates ($w_R = 87.03\%$, $w_P < 0.01\%$) in the reactant-well region near $s_R = 3.0$ Å, whereas the P structure dominates ($w_P = 88.05\%$, $w_R < 0.01\%$) in the product-well region near s_P. As one approaches the transition state (TS) region from either side, the weightings $w_R(s)$ and $w_P(s)$ of the two resonance structures gradually approach equality, until they cross ($w_R = w_P$) near the TS. We may designate the crossing point $s^\ddagger_N$ at which

$$w_R(s^\ddagger_N) = w_P(s^\ddagger_N) \tag{8.2}$$

as the ''natural transition state'' (NTS), to distinguish it from the corresponding point ($s^\ddagger$) at the top of the energy barrier [where the NRT weightings are found to be $w_R(s^\ddagger) = 48.4\%$, $w_P(s^\ddagger) = 31.3\%$]. In the present case, the NTS is found to occur near $s^\ddagger_N = 2.078$ Å, differing only slightly from $s^\ddagger$. On physical and chemical grounds, the approximation $s^\ddagger_N \simeq s^\ddagger$ would be expected to hold true for many chemical reactions.

Figure 3c shows the corresponding variations of NRT bond orders for the four distinct CC bonds (in conventional cyclohexene numbering, b_{12}, b_{23}, b_{34}, b_{45}). Consistent with the expected chemical picture, these evolve continuously from the (1, 2, 0, 2) pattern of the reactant structure to the (2, 1, 1, 1) pattern of the product structure, with an approximate (1.5, 1.5, 0.5, 1.5) pattern at the TS. Although the quantitative values of the NRT bond orders and weightings will be altered in higher level treatments of the reaction profile (particularly, inclusion of correlation effects), the chemically reasonable variations shown in Figure 3a–c

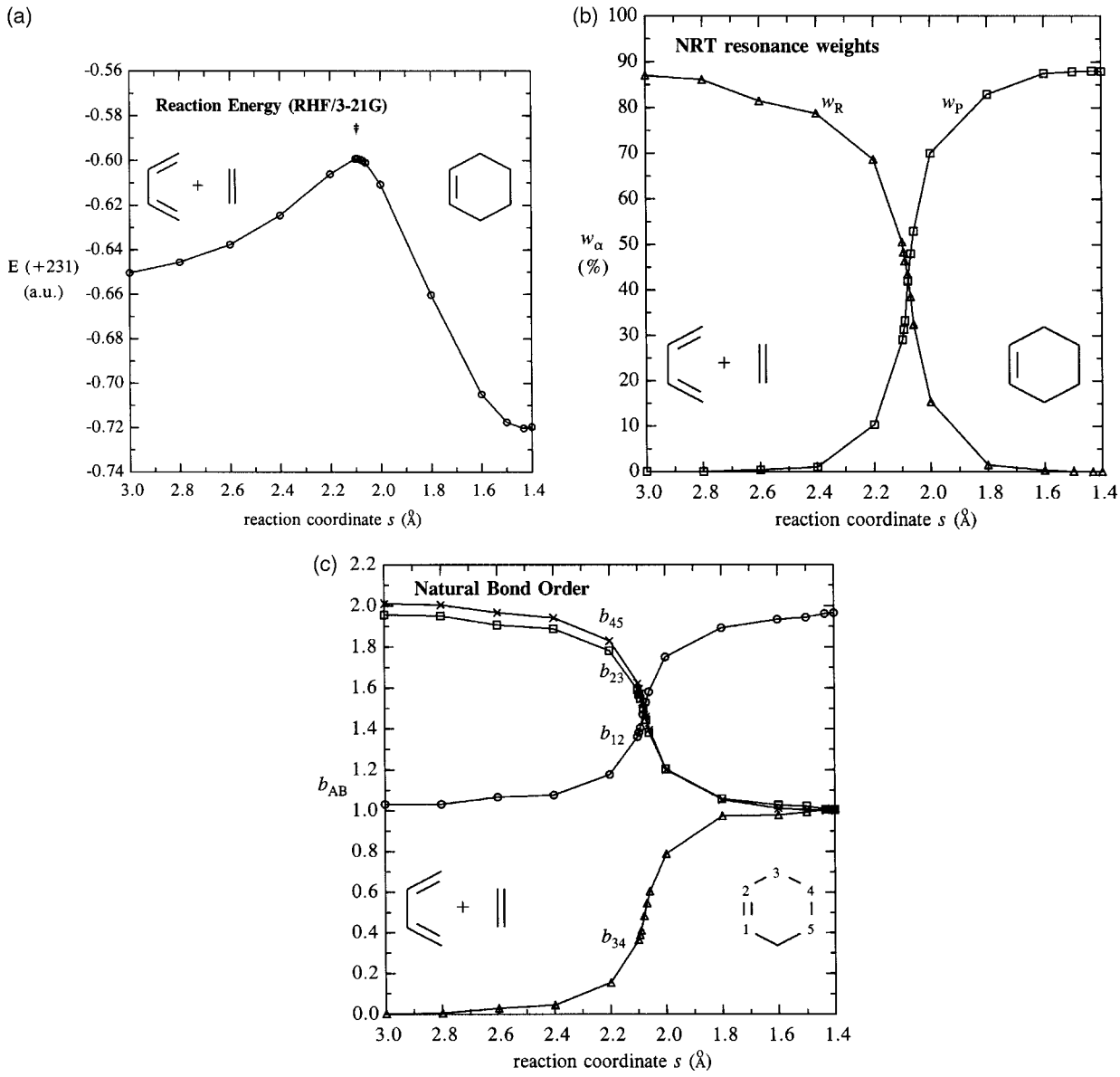

FIGURE 3. (a) Reaction energy profile for model Diels-Alder reaction,

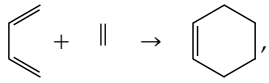

calculated at RHF / 3-21G level (see text for geometry and definition of reaction coordinate *s*). (b) NRT resonance weights for reactant (w_R; triangles) and product (w_P; squares) resonance structures along the model Diels-Alder reaction coordinate. (c) Natural bond order b_{AB} along the reaction coordinate, showing the evolution from reactant (butadiene plus ethylene) to product (cyclohexene) bond patterns. Bond numbering corresponds to cyclohexene labelling (e.g., b_{12} is the final cyclohexene double bond and b_{45} the initial ethylene double bond).

are expected to be preserved at higher theoretical levels.

Figure 4 compares the NRT bond orders to optimized CC bond lengths for all points along the Diels-Alder reaction coordinate. The values of R_{CC} and b_{CC} are highly correlated and appear to lie along a universal smooth curve. The nonlinear "kinks" of this curve are consistent with the expectation [cf. (3.9) in the preceding paper] that a bond order–bond length curve cannot be globally

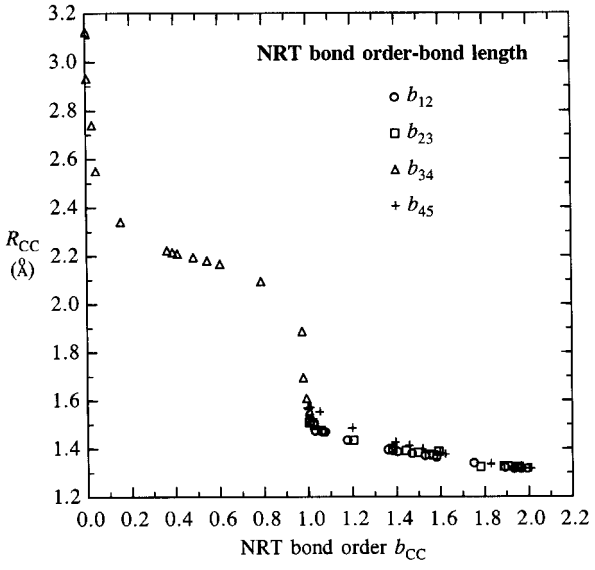

FIGURE 4. NRT bond order–bond length correlation for CC bond variations along the model Diels-Alder reaction coordinate (cf. Fig. 3a–c).

linear. Nevertheless, there are conspicuous broad regions (e.g., centered about $b_{CC} = 0.5, 1.5$) where a linear bond order–bond length assumption is apparently well justified. The global NRT bond order–bond length curve[42] of Figure 4 is therefore qualitatively consistent with empirical Pauling-Wheland correlations, but the quantitative form of this curve should considerably extend the predictive power of such correlations.

Summary and Conclusions

The natural resonance theory (NRT) method provides a new, quantitative tool to express the chemical content of numerical wave functions in the familiar and intuitive language of resonance theory. Unlike classical Pauling-Wheland theory, the NRT method makes no reference to ''valence bond,'' multiconfigurational, or other specialized form of wave function. Rather, it employs only the information contained in the first-order reduced density matrix and is therefore applicable to any *ab initio* or semiempirical quantum chemical procedure (including variational, Møller-Plesset perturbative, and density functional methods) for which a density matrix is available. The NRT method has been implemented as a general-purpose program[7] (embedded in the general Natural Bond Orbital analysis package[43] that can be attached to a wide variety of modern electronic structure systems, including Gaussian 9X,[44] GAMESS,[45] and others. In the present paper, we have emphasized NRT applications in the framework of *ab initio* molecular orbital theory in order to demonstrate the practicality of NRT analysis for the most widely used quantum chemical methods and its independence from VB-type wave functions.

The results presented here illustrate the NRT description for a wide variety of chemical species: cyclic and acyclic; neutral and charged; symmetric and nonsymmetric; and hypervalent, hypovalent, normal covalent, ionic, coordinate covalent, and noncovalent bonding types. Emphasis has been placed on some classical applications of resonance theory (benzene, CO_2, amide group, carboxylate ion, etc.) as well as nonconventional applications to subtle bond fixing (Mills-Nixon), torsional, H bonding, and conjugative coupling effects. The former applications serve to demonstrate the broad consistency of NRT analysis with conventional Pauling-Wheland concepts (despite important differences, e.g., in the treatment of ''ionic-covalent resonance''). The latter serve to illustrate the many extensions and refinements of resonance-theoretic reasoning that become feasible in the quantitative NRT framework. We have also demonstrated the applicability of NRT analysis to the continuous chemical transformations of a model Diels-Alder reaction, relating the transition state to the competing reactant and product resonance structures. Our emphasis throughout has been on sampling a broad range of NRT applications, rather than investigating particular systems in detail. We believe that these examples provide a useful baseline for future NRT investigations of a wide variety of organic, inorganic, and biochemical systems.

Resonance theory once represented the most dominant influence in theoretical chemistry. We believe it can once again play an active, creative role in modern chemistry, infused with a new degree of quantitative *ab initio* rigor and generality.

Appendix

The minimum of the NRT variational functional [eq. (4.7) in the first accompanying paper] can be derived *exactly* for the elementary case of the benzene pi system in a minimal basis (e.g., Hückel-type) framework, where the pi MOs are determined by symmetry. When these MOs are transformed to a basis of localized bond (π_i) and

antibond (π_i^*) NBOs (i = 1, 2, 3), it is readily shown that the π_i and π_i^* occupancies $q_i = \langle \pi_i | \hat{\Gamma} | \pi_i \rangle$, $q_i^* = \langle \pi_i^* | \hat{\Gamma} | \pi_i^* \rangle$ are given by

$$q_1 = q_2 = q_3 = 1\tfrac{2}{3},\ q_1^* = q_2^* = q_3^* = \tfrac{1}{3}. \quad \text{(A1)}$$

For the usual covalent resonance structures [Kekulé structures K (reference), K′; Dewar structures D1, D2, D3], one can readily write out the table of occupancies $q_{i\alpha}$ of π_i and π_i^* NBOs as shown below.

NBO	K	K′	D1	D2	D3	true
π_1^*	0	1	1	1	0	$\frac{1}{3}$
π_2^*	0	1	1	0	1	$\frac{1}{3}$
π_3^*	0	1	0	1	1	$\frac{1}{3}$
π_1	2	1	2	2	0	$1\frac{2}{3}$
π_2	2	1	2	0	2	$1\frac{2}{3}$
π_3	2	1	0	2	2	$1\frac{2}{3}$

If we choose the weights of the three Dewar structures to be identical (w_D), the differences

$$q_i - \sum_\alpha w_\alpha q_{i\alpha}$$

are seen to be

$$\tfrac{1}{3} - w_{K'} - 2w_D, \text{ for each } \pi_i^* \quad \text{(A2)}$$

$$1\tfrac{2}{3} - 2w_K - w_{K'} - 4w_D, \text{ for each } \pi_i. \quad \text{(A3)}$$

With the normalization condition $w_K + w_{K'} + 3w_D = 1$, one can eliminate w_K from (A3) to see that (A2) and (A3) are equivalent. Thus, there are two independent unknowns to satisfy a single condition (A2), and the variational minimum $d(w_{K'}, w_K, w_D) = 0$ (corresponding to $f(\underline{w}) = 1$) is achieved for any values of $w_{K'}$, w_D satisfying (A2). In particular, the weights $w_K = \frac{2}{3}$ and $w_{K'} = \frac{1}{3}$ for the two Kekulé structures reproduce the benzene pi occupancies (A1) exactly, with no contribution from Dewar structures ($w_D = 0$).

Acknowledgments

We thank Prof. J. C. Weisshaar for many discussions relating to benzyl cation and aromatic methyl rotors, Dr. Jens Abildgaard for suggesting the example of malonaldehyde, and Prof. Paul v.R. Schleyer for many helpful critical suggestions. A grant of RS/6000 computers from the IBM Corporation and other computational support provided by the NSF grant CHE-9007850 are gratefully acknowledged.

References

1. L. Pauling, in A. R. Todd (ed.), *Perspectives in Organic Chemistry*, Wiley Interscience, New York, 1956.
2. G. W. Wheland, *Resonance in Organic Chemistry*, John Wiley and Sons, New York, 1955.
3. L. Pauling and F. W. Wheland, *J. Chem. Phys.*, **1**, 362 (1933); H. Eyring, J. Walter, and G. E. Kimball, *Quantum Chemistry*, Wiley, New York, 1944, pp. 249–254.
4. L. Pauling, *The Nature of the Chemical Bond*, 3rd ed., Cornell University Press, Ithaca, NY, 1960.
5. For an authoritative description of standard *ab initio* computational methods and basis set designations referred to herein, see W. J. Hehre, L. Radom, P. v. R. Schleyer, and J. A. Pople, *Ab Initio Molecular Orbital Theory*, Wiley, New York, 1986.
6. J. A. Pople and M. S. Gordon, *J. Am. Chem. Soc.*, **89**, 4253 (1967).
7. F. Weinhold, *NBO 4.0 Program Manual*, University of Wisconsin Theoretical Chemistry Institute, Madison, 1994, Sect. B.8; J. K. Badenhoop, *Ph.D. Thesis*, University of Wisconsin, Madison, 1994.
8. E. D. Glendening, R. Faust, A. Streitwieser, K. P. C. Vollhardt, and F. Weinhold, *J. Am. Chem. Soc.*, **115**, 10952 (1993).
9. Throughout this paper, ''formal charge'' labels are attached to assist in specifying the complete Lewis structure for cases that may otherwise be ambiguous. We typically omit specification of lone pairs unless highlighted in the discussion. Note that ''formal charges'' are purely a notational device, only loosely connected to the physical charge distribution as described, e.g., by natural population analysis. Note also that when two electronically distinct ''structures'' (corresponding, in the case of CO_2, to the two twisted orientations of orthogonal pi bonds) map onto a *single* Lewis diagram, as in (3.1a), the diagram is labelled with their combined weight (49.7%). However, multiple *equivalent* Lewis diagrams are specified by giving the calculated weighting for one member of the set, followed by the multiplicity in parentheses, as for the two equivalent triple-bonded structures (3.1b).
10. Strong resonance mixing is also observed for non-D_{6h} geometries that break the symmetry equivalence of the two Kekulé structures in (1.1). In contrast, for the cyclobutadiene ''analog'' (1.2), there is *no* resonance mixing of the two structures in geometries that differ even infinitesimally from D_{4h} symmetry (corresponding to the fact that $\pi \rightarrow \pi^*$ NBO delocalizations are rigorously absent in this case; see below).
11. For brevity's sake, in the following, we display only the leading resonance structure contributions, showing all reference structures [bracketed] and, in some cases, the few most important secondary structures. Although the weights of neglected structures are generally significantly smaller than those displayed, their cumulative contribution can be appreciable, as, e.g., in (2.7). Additional details of neglected structures are available from the authors.

12. K.-T. Lu, G. C. Eiden, J. K. Badenhoop, F. Weinhold, and J. C. Weisshaar, in, T. Baer, C. Ng, and I. Powis (eds.), *Current Topics in Ion Chemistry and Physics*, *Vol. IV: Highly Resolved Laser Photoionization and Photoelectron Studies*, Wiley, New York, 1994.
13. W. H. Mills and I. G. Nixon, *J. Chem. Soc.*, **1930**, 2510 (1930); reference 4, pp. 201–202.
14. As the idealized ''PG-like'' geometry for this species, we used the idealized geometry of neutral toluene, with the methyl group replaced by a planar trigonal CH_2 group (R_{CH} = 1.09 Å, R_{CC} = 1.52 Å).
15. G. C. Eiden, F. Weinhold, and J. C. Weisshaar, *J. Chem. Phys.*, **95**, 8665 (1991).
16. In optimized geometry, the quinone-like structure (2.7b) becomes more highly weighted (w_b = 16.9%) than either Kekulé structure (w_a = 9.9% each), with polar structures (2.7c) intermediate (w_c = 14.1% each), further accentuating the quinone-like NRT description (b_{1x} = 1.5966, b_{12} = 1.1563, b_{23} = 1.5419, b_{34} = 1.3376).
17. See, e.g., R. T. Morrison and R. N. Boyd, *Organic Chemistry*, 3rd ed., Allyn & Bacon: Boston, 1973, p. 989.
18. See reference 4, pp. 267–269.
19. Note, however, that more quantitative comparisons of two systems should be based on a common number of comparable reference structures. [For example, (3.2) can be compared directly with (3.1), but not with (3.3); the latter involves a smaller set of reference structures.] The $NRTSTR keylist can be used to stipulate a comparable set of reference structures (see, e.g., the examples in the penultimate text section) when the default reference structures for two molecules are dissimilar.
20. In the Pauling-Wheland ''covalent-ionic resonance'' formalism, each structure in (3.5) would therefore correspond to significant contributions from more highly ionic structures, such as

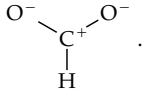

21. A more comprehensive discussion of the important topic of resonance in amides and related groups is reserved for a forthcoming paper.
22. See, e.g., C. A. Coulson, *Valence*, Oxford University Press: London, 1961, pp. 128–138; reference 4, Section 3.1; J. Braunstein and W. T. Simpson, *J. Chem. Phys.* **23**, 176 (1955). The notion of a fundamental dichotomy between ionic and covalent ''types'' (espoused by Langmuir, Sidgwick, and Sugden) was opposed by Lewis, Mulliken, and others; see the general historical discussion in Jensen (reference 25), pp. 74–77.
23. T. K. Brunck and F. Weinhold, *J. Am. Chem. Soc.*, **101**, 1700 (1979); A. E. Reed and F. Weinhold, *Isr. J. Chem.*, **31**, 277 (1991).
24. In Pauling-Wheland theory, the origins of internal rotation barriers were not linked to resonance interactions such as (4.2), but instead were attributed to *d*- and *f*-orbital contributions to bonding hybrids (reference 4, pp. 130–134).
25. W. B. Jensen, *The Lewis Acid–Base Concepts*, Wiley, New York, 1980; H. A. Bent, *Chem. Rev.*, **68**, 587 (1968); see also references 27 and 36.
26. P. J. Hay and W. R. Wadt, *J. Chem. Phys.*, **82**, 270 (1985).
27. See, e.g., F. A. Cotton and G. Wilkinson, *Advanced Inorganic Chemistry*, Wiley, New York, 1962, pp. 614–617.
28. R. E. Rundle, *Rec. Chem. Progr.*, **23**, 195 (1962); K. S. Pitzer, *Science*, **139**, 414 (1963); J. I. Musher, *Angew. Chem.* **81**, 68 (1969).
29. A. E. Reed and F. Weinhold, *J. Am. Chem. Soc.*, **108**, 3586 (1986).
30. Structure (6.2b) is associated with *d* bonding, as evidenced by the fact that this structure is absent in the corresponding RHF/6-31G calculation where *d* orbitals are lacking.
31. L. Suidan, J. K. Badenhoop, E. D. Glendening, and F. Weinhold, *J. Chem. Educ.*, **72**, 583 (1995).
32. G. N. Lewis, *J. Chem. Phys.*, **1**, 17 (1933); W. N. Lipscomb, *J. Chem. Phys.*, **22**, 985 (1954); D. S. Jones and W. N. Lipcomb, *Acta Crystallogr.* **26**, 196 (1970); W. N. Lipscomb, *Boron Hydrides*, W. A. Benjamin, New York, 1963, Chapters 2, 3.
33. See, e.g., reference 4, p. 369. Pauling considers three types of BB-bonded structures (''C, D, E'') in addition to those (''A, B'') of the NRT expansion, with uncertain relative weightings (various estimates are presented that differ by a factor of three). The NRT bond order (b_{BB} = 0.0102) shows no evidence for significant metal–metal bonding.
34. L. Pauling, *Proc. Natl. Acad. Sci. USA*, **14**, 359 (1928); *J. Am. Chem. Soc.*, **53**, 1367 (1931).
35. G. N. Lewis, *Valence and the Structure of Atoms and Molecules*, Chemical Catalog Co.: New York, 1923, especially the section ''Bivalent Hydrogen.'' Lewis dot structures for water dimer and FHF^- (expressing the partial sharing of electron pairs with two atoms) were included in the first discussions of H bonding: M. L. Huggins, Thesis, University of California, Berkeley, 1919; W. M. Latimer and W. H. Rodebush, *J. Am. Chem. Soc.*, **42**, 1419 (1920).
36. N. V. Sidgwick, *The Electronic Theory of Valency*, Clarendon Press, Oxford, 1927.
37. C. A. Coulson, *Research*, **10**, 149 (1957).
38. A. E. Reed, L. A. Curtiss, and F. Weinhold, *Chem. Rev.*, **88**, 899 (1988).
39. A. E. Reed and F. Weinhold, *J. Chem. Phys.*, **78**, 4066 (1983); L. A. Curtiss, D. J. Pochatko, A. E. Reed, and F. Weinhold, *J. Chem. Phys.*, **82**, 2679 (1985); A. E. Reed, F. Weinhold, L. A. Curtiss, and D. Pochatko, *J. Chem. Phys.*, **84**, 5687 (1986); P. Seiler, G. R. Weisman, E. D. Glendening, F. Weinhold, V. B. Johnson, and J. D. Dunitz, *Angew. Chem.* (*Engl. Ed.*), **26**, 1175 (1987).
40. T. Chiavassa, P. Roubin, L. Pizzala, P. Verlaque, A. Allouche, and F. Marinelli, *J. Phys. Chem.*, **96**, 10659 (1992); Z. Latajka and S. Scheiner, *J. Phys. Chem.*, **96**, 9764 (1992).
41. Z. K. Smedarchina and W. Siebrand, *J. Mol. Struct.*, **297**, 207 (1993); S. J. Formosinho and L. G. Arnaut, *J. Photochem. Photobiol.*, **A75**, 21 (1993); E. B. Wilson and Z. Smith, *Acc. Chem. Res.*, **20**, 257 (1987), and references therein.
42. Of course, b_{AB} vs. R_{AB} curves differ quantitatively for different A—B bond types. In particular, there is no à priori reason to assume that bond length changes for C—C bonds are equal to those of, e.g., C—O or C—N bonds for comparable bond order changes. It is also known that A—B bond lengths depend significantly on hybridization [viz., $C(sp^3)$—H vs. $C(sp^2)$—H], atomic charge, ring geometry

constraints, and other factors not directly related to resonance delocalization, and thus not reflected in bond order variations.

43. E. D. Glendening, A. E. Reed, J. E. Carpenter, and F. Weinhold, *QCPE Bull.*, **10**, 58 (1990); *NBO 3.0 Program Manual*, University of Wisconsin Theoretical Chemistry Institute Technical Note WIS-TCI-756, Madison, 1990.
44. M. J. Frisch, G. W. Trucks, M. Head-Gordon, P. M. W. Gill, M. W. Wong, J. B. Foresman, B. G. Johnson, H. B. Schlegel, M. A. Robb, E. S. Repogle, R. Gomperts, J. L. Andres, K. Raghavachari, J. S. Binkley, C. Gonzalez, R. L. Martin, D. J. Fox, D. J. Defrees, J. Baker, J. J. P. Stewart, and J. A. Pople, *Gaussian 92*, *Revision A*, Gaussian, Inc., Pittsburgh, 1992.
45. *GAMESS* version March 1992: M. W. Schmidt, K. K. Baldridge, J. A. Boatz, J. H. Jensen, S. Koseki, M. S. Gordon, K. A. Nguyen, T. L. Windus, and S. T. Elbert, *QCPE Bull.*, **10**, 52 (1990).